

# Synthetic Geology - Structural Geology Meets Deep Learning

Simon Ghyselincs<sup>1</sup>, Valeriia Okhmak<sup>3</sup>, Stefano Zampini<sup>3</sup>, George Turkiyyah<sup>3</sup>, David Keyes<sup>3</sup>, and Eldad Haber<sup>2,\*</sup>

<sup>1</sup>Department of Engineering Physics, University of British Columbia

<sup>2</sup>Department of Earth, Ocean and Atmospheric Sciences, University of British Columbia

<sup>3</sup>Division of Computer, Electrical and Mathematical Sciences and Engineering, King Abdullah University of Science and Technology

\*eldad.haber@ubc.ca

## ABSTRACT

Visualizing the first few kilometers of the Earth's subsurface, a long-standing challenge gating a virtually inexhaustible list of important applications, is coming within reach through deep learning. Building on techniques of generative artificial intelligence applied to voxelated images, we demonstrate a method that extends surface geological data supplemented by boreholes to a three-dimensional subsurface region by training a neural network. The Earth's land area having been extensively mapped for geological features, the bottleneck of this or any related technique is the availability of data below the surface. Drilling is expensive and generally confined to regions where recovery of minerals, petroleum, water, thermal energy, or other marketable commodities is economical. We close this data gap in the development of subsurface deep learning by designing a synthetic data-generator process that mimics eons of geological activity such as sediment compaction, volcanic intrusion, and tectonic dynamics to produce a virtually limitless number of samples of the near lithosphere. A foundation model trained on such synthetic data is able to generate a 3D image of the subsurface from a previously unseen map of surface topography and geology, showing increasing fidelity with increasing access to borehole data, depicting such structures as layers, faults, folds, dikes, and sills. We illustrate the early promise of the combination of a synthetic lithospheric generator with a trained neural network model using generative flow matching. Ultimately, such models will be fine-tuned on data from applicable campaigns, such as mineral prospecting in a given region. Though useful in itself, a regionally fine-tuned models may be employed not as an end but as a means: as an AI-based regularizer in a more traditional inverse problem application, in which the objective function represents the mismatch of additional data with physical models with applications in resource exploration, hazard assessment, and geotechnical engineering.

## Introduction

Structural geology focuses on the deformation and motion of rocks in the Earth's crust, describing three-dimensional distributions of rock formations and structures to understand the processes that shape the crust<sup>1,2</sup>. Structural geologists use a variety of techniques and methods to investigate and interpret these features, including field mapping, structural analysis of rock outcrops, laboratory experiments, remote sensing, and geophysical imaging. The insights gained are essential for understanding the evolution of mountain ranges, the formation of mineral and energy resources, and the assessment of geological hazards such as earthquakes and landslides, among other fundamental aspects of Earth science.

The construction of accurate structural geological models from collected data is a complex, ill-posed problem fraught with challenges (see, e.g.,<sup>3</sup> and references within). These models must reconcile geological observations obtained from what are often sparse and incomplete sources such as field data, rock samples, geophysical surveys, and remote sensing. Geological data is subject to uncertainty and interpretation, posing significant challenges in quantifying and addressing errors within the model<sup>4</sup>. The interpretation of uncertain data is further exacerbated by the intricate and heterogeneous nature of geological structures, which unfold over diverse spatial and temporal scales—ranging from microscopic mineral deformation to regional tectonic movements spanning millions of years<sup>5</sup>. Integrating disparate datasets and models from multiple disciplines, including structural geology, geophysics, and geochemistry, represents an additional hurdle that demands interdisciplinary collaboration<sup>6</sup>.

Overcoming these challenges requires innovative technologies, advanced analytical methods, and interdisciplinary collaboration. However, the rewards of overcoming these obstacles are substantial, as accurate and reliable structural geological models are indispensable for understanding Earth's subsurface processes, predicting geological hazards, and managing natural resources. Traditionally, the construction of 3D structural geological models has been a manual, labor-intensive process, relying on expert interpretation, visualization, and iterative refinement of multiple data sources<sup>7-9</sup>. Such manual workflows can take

many hours and usually produce a single deterministic model, ignoring the underlying ill-posedness of the problem.

In this study, we take a step toward automating structural geology modeling by leveraging generative artificial intelligence (GAI) techniques. First, we create a geologically plausible, infinite synthetic structural dataset that reflects the diverse processes and events shaping the Earth’s crust. This dataset is then used to train a 3D GAI model with flow matching<sup>10,11</sup>. Unlike traditional deterministic methods, this approach allows for the generation of multiple plausible models, capturing a richer range of potential subsurface scenarios.

Once trained, the generative model can be integrated with other conditional data and applied to various geological tasks. For example, it can be coupled with information obtained from drilling or surface measurement, geostatistical interpolation, or geological segmentation that incorporates geological priors, improving model reliability and reducing ambiguity in subsurface interpretations. We demonstrate this capability through experiments on the reconstruction of geological stratigraphy from sparse geological data, illustrating the potential of generative models to advance structural geology research and practice.

## Methods

### Synthetic Dataset

Recent advances in generative diffusion models capable of strikingly realistic images (see, e.g.,<sup>11,12</sup> and references within) have both motivated and been fueled by the compilation of ever-expanding, detailed training datasets (e.g., Imagenet<sup>13</sup>). However, for 3D geological data, no comparable large-scale training sets exist, partly because we cannot directly observe high-resolution, three-dimensional underground rock formations. Consequently, one of the primary obstacles to creating a geological training set for 3D GAI is acquiring comprehensive samples that reflect the wide variety of possible features and configurations that are present in the Earth’s crust<sup>14</sup>. To address this gap in information, we generate a synthetic dataset that captures the fundamental principles of structural geology that have been amassed through research and field observation. The ideal synthetic data for deep learning should simulate empirically drawn, independent, and identically distributed (i.i.d.) samples from the set of all 3D volumes in the Earth’s crust. A deep generative model aims to learn a representation of the underlying probability distribution of geological structures from the samples, either implicitly or explicitly, in order to generate new samples that have never been seen before<sup>15,16</sup>.

The difficulty of obtaining true observational data extends beyond geology, affecting other domains in scientific machine learning; fluid flow<sup>17</sup>, wave simulation<sup>18</sup>, and biology<sup>19</sup> share similar challenges. Moreover, progressively more complex large language models are predicted to run out of sufficient training data in the future<sup>20</sup>. In these cases, it has been suggested that numerical simulations or synthetic data are used to either generate or augment the data that is needed to train a generative model. These simulations can produce abundant, high-resolution data at large scales, yet also carry the risk that the generated data has some implicit bias and does not correctly represent the true distribution. Nevertheless, such theoretical frameworks represent our best current knowledge about the particular field of interest, making them highly useful for explaining indirect measurements.

In response to these constraints, we adopt a geomodel-driven approach<sup>4</sup>, bootstrapping an initial synthetic dataset through classical simulation methods based upon fundamental principles of how stratigraphic layers form over long time spans. We compile sequential, parameterized geological processes and workflows via mesh- and grid-based numerical techniques. These simulations are frequently used to explain observed geological formations, making them well-suited for creating synthetic data.

Current open-source 3D modeling efforts have been led by tools such as GemPy<sup>21</sup>, Noddy<sup>22,23</sup>, and LoopStructural<sup>24</sup>, producing 3D geological volumes using a set of informed and constrained parameters to model limited underlying geological processes over time. While these tools are invaluable in their respective scopes of use, they do not natively support large-scale randomization. For example, Jessell et al.<sup>23</sup> have suggested that more parameters, more events, linked events, and more models would improve their existing efforts. We thus adopt a computational method suggested in Visible Geology<sup>25</sup>, where geological processes are represented as mathematical transformations of a 3D mesh. By combining multiple transformations, one can generate a wide range of realistic geological models. In fact, such models are used to train geologists<sup>25</sup>, suggesting their suitability as a synthetic dataset for training machine-learning models. Additionally, randomizing and reordering these processes enables the generation of a virtually limitless number of 3D volumes depicting complex and varied geology. We implement this randomized workflow in the open-source Python package *StructuralGeo*.

### Sample Generation

Geological model training data samples, referred to as Geomodels, take the form of 3D tensors denoted as  $\mathbf{m}(\mathbf{x}) : R^3 \rightarrow \mathbb{N}$ ,  $\mathbf{x} = [\mathbf{x}_1, \mathbf{x}_2, \mathbf{x}_3]$  and  $\mathbb{N} = \{1, \dots, N\}$ . Each element of the tensor  $\mathbf{x}$  corresponds to a voxel in a 3D mesh grid, with an integer label (from  $1, \dots, N$ ) indicating its assigned rock-strata category. The data is composed of discrete categorical values, which are representative of the labeling and segmentation that a geologist would apply to collected field data.

We define two classes of processes acting on  $\mathbf{x}$  :

1. *Transformations*  $\mathcal{T} : R^3 \rightarrow R^3$  which transport or displace the geological medium, and
2. *Depositions*  $\mathcal{D} : R^3 \rightarrow \mathbb{N}$  which modify the composition.

**Transformations:** Transformations ( $\mathcal{T}$ ) are general operations that deform, rotate, or otherwise displace the geological medium according to parameters  $\theta$ . Let  $\mathbf{u}(\mathbf{x}; \theta) : R^3 \rightarrow R^3$  be a vector-valued function dependent on  $\theta$ . A single transformation  $\mathcal{T}_\theta$  is then expressed as a coordinate mapping, that is

$$\mathcal{T}_\theta(\mathbf{m}(\mathbf{x})) = \mathbf{m}(\mathbf{x} + \mathbf{u}(\mathbf{x}; \theta)). \quad (1)$$

Transformations describe many geological processes ranging from folding to shearing and are combined to create complex deformations. However, they are insufficient if we consider the need to introduce or remove geological materials from the Geomodel domain, for which we use deposition events.

**Depositions:** Depositions ( $\mathcal{D}$ ) add or remove material into the model domain through sedimentation, erosion, or intrusion events; for example, the transport of hot fluids from the interior of the Earth through a fissure. In a deposition, we envision some material (new rock) that replaces existing rock by pushing it aside, eroding it away, or accumulating above it. The extent and nature of a deposition event are controlled by a set of parameters  $\theta$ . A simple mathematical model uses a window function  $\mathbf{w}(\mathbf{x}, \theta)$  that has the value 1 where the deposition occurs and 0 otherwise. This function is generated by first considering a canonical window

$$\mathbf{w}_0(\mathbf{x}) = \prod_{i=1}^3 (H(\mathbf{x}_i + 1) - H(\mathbf{x}_i - 1)),$$

where  $H$  is the Heaviside function. We then map  $\mathbf{w}_0(\mathbf{x})$  using a transformation  $\mathcal{T}_\theta$  to allow scaling, rotations, translations, and bending, that is

$$\mathbf{w}(\mathbf{x}, \theta) = \mathcal{T}_\theta(\mathbf{w}_0(\mathbf{x})). \quad (2)$$

Given a Geomodel  $\mathbf{m}(\mathbf{x})$  and a category label  $a$ , the deposition process is defined by

$$\mathcal{D}_\theta(\mathbf{m}, a) = (1 - \mathbf{w}(\mathbf{x}, \theta)) \mathbf{m}(\mathbf{x}) + a \mathbf{w}(\mathbf{x}, \theta). \quad (3)$$

Hence,  $\mathbf{m}(\mathbf{x})$  is overwritten by the new category  $a$  wherever  $\mathbf{w}(\mathbf{x}, \theta) = 1$ .

**Geological Histories:** A complete Geomodel is constructed by combining both transformation ( $\mathcal{T}$ ) and depositions ( $\mathcal{D}$ ) to simulate geological evolution over discrete time steps. The initial state of the Geomodel is described by a mapping  $\mathbf{m}_0(\mathbf{x})$ , which depends only on the vertical axis  $\mathbf{x}_3$ , thus forming sequential horizontal layers. Next, multiple transformations and depositions (e.g., folding, dike formation, shearing), each with its parameters  $\theta$ , are sequenced together to form a more complex history. Let  $\mathcal{P}^i$  represent a generic geological process (either ( $\mathcal{T}$ ) or ( $\mathcal{D}$ )). The complete history is simply a composition of many such processes, that is

$$\mathbf{m}(\mathbf{x}) = \mathcal{H}(\mathbf{m}_0) = \mathcal{P}^n \circ \dots \circ \mathcal{P}^{i+1} \circ \mathcal{P}^i \dots \circ \mathcal{P}^1(\mathbf{m}_0(\mathbf{x})). \quad (4)$$

To numerically evaluate the model  $\mathbf{m}(\mathbf{x})$  under transformations and depositions, we use backward interpolation, common in image transformation problems<sup>26</sup>. Figure 1 illustrates one example of such a history.

Although the Geomodel equation 4 is deterministic once the sequence and parameters are fixed, we introduce variability using a Markov chain to sequence new histories, drawing from the set of all possible geological processes  $\{\mathcal{P}^j\}, j = 1, \dots, k$ . After each process, the next is chosen with some probability

$$\pi_j = \pi(\mathcal{P}^j | \mathcal{P}^{j-1}), \quad (5)$$

conditioned on the previous event. This yields a random geological history for the computational sequence in equation 4. Termination occurs when a special end-of-process token is drawn; hence, models emerge as random computational sequences of variable length. Because each process has its randomized parameters, repeated runs produce diverse realizations with high variability in both the ordering of events and overall geological age. Figure 2 provides an overview of the generation pipeline.

The above simulation can generate a virtually infinite number of geological models with variable complexity and at any specified resolution, which can be used as data for a generative model. Nonetheless, just like any other simulation, it depends on a number of hyperparameters that need to be carefully tuned. Every geological process depends on a set of parameters that are sampled as random variables and must be tuned such that the outcome of each geological process is "realistic" as visually determined by geologists. In addition, the transition probability  $\pi_j$  of every geological process must be chosen such that it yields a reasonable geology as judged by a domain expert. However, it is important to realize that such models represent what experts consider to be unbiased geology. Since there are no direct observations on the geology at the (3D) resolution and scale that we need, it is virtually impossible to know if such models introduce implicit bias. Nonetheless, such models are extremely useful in generating what experts believe is a realistic Earth model.

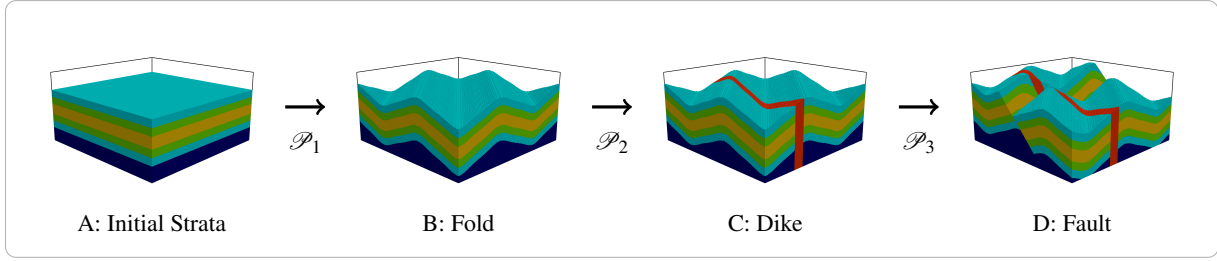


**Figure 1.** An example of geological history illustrating the application of transformations and depositions. (A) The initial strata  $\mathbf{m}_0(\mathbf{x})$ , (B) folded by a transformation  $\mathcal{T}_{\text{fold}}$ , (C) intruded by a dike  $\mathcal{D}_{\text{dike}}$ , and (D) finally faulted by another transformation  $\mathcal{T}_{\text{fault}}$ . Each arrow represents a process  $\mathcal{P}_i$  in the overall history  $\mathcal{H}$ . In practice, these processes are sequenced randomly from a set  $\mathcal{P}_j, j = 1, \dots, k$  using a Markov chain, leading to varied geological outcomes.

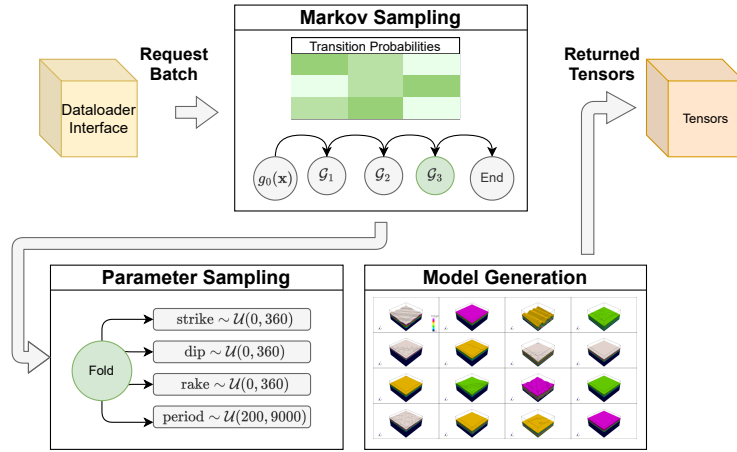


**Figure 2.** Illustration of the pipeline for random geological model generation. A batch request triggers a Markov chain sampler, which selects and sequences geological processes (e.g., folding, deposition) from a transition matrix. For each process, parameters such as amplitude and wavelength are drawn from tuned random variables. Finally, the constructed computational sequences are applied to produce multiple models in the form of 3D tensors.

### Synthetic Geology Using Generative AI

Let  $\mathbf{m}(\mathbf{x})$  be a geological model generated by the simulation process using a sampled geological history  $\mathcal{H}(\mathbf{m}_0)$ . These models reside in a high-dimensional probability space  $\pi_m$  covering the range of all possible 3D geological structures.

Given a method to generate virtually infinite samples of Geomodels,  $\mathbf{m}(\mathbf{x})$ , we now have the required tools to train a foundation model to learn the probability of any given Geomodel,  $\pi_m(\mathbf{m})$  or its associated score function defined as,  $s_m = -\nabla_m \log(\pi_m(\mathbf{m}))$ .

A natural question arises: what are the key advantages and practical applications of learning the distribution  $\pi_m$  associated with the synthetic generative process described earlier? That is, how does the ability of a foundation model to estimate  $\pi_m$  enhance our understanding or extend our capabilities, given that we already have a method of generating such samples?

While the original simulation process can generate diverse Geomodels, it is hard, and in some cases virtually impossible, to use the simulation for any other application besides the forward process of generating a random 3D geological volume from a parameterized history  $\mathcal{H}(\mathbf{m}_0)$ . In contrast, foundation models support a broader range of applications that vary from generation to conditional generation or inversion, enabling the incorporation of other data or constraints based on conditional distributions<sup>27</sup>.

For instance, while the simulation process requires a structured history of geological events, a foundation model can generate realistic samples conditioned directly on partial observations in the spatial domain  $\mathbf{x}$ , such as borehole data or surface measurements. Since our ultimate goal is to fuse multiple sources of geo-scientific data, we seek to replace the rigid simulation process with a flexible, trainable foundation model.

One approach to learning a probability density function  $\pi_m$  is the denoising or diffusion model, now commonly used for image and movie generation. While diffusion methods are often applied to continuous-valued data, the generation of

discrete-valued data has only more recently been addressed<sup>28</sup> through the theory first proposed by Hyvärinen<sup>29</sup>. One of the difficulties with score matching for our application is the fact that the score does not exist for discrete distributions. A more general way to approach the problem of matching distributions that does not require the score can be derived through flow matching<sup>10</sup>.

**Embedding Discrete Categorical Data** To adapt flow matching to discrete categorical data, we reformulate the problem by embedding the data into a continuous space without imposing any inherent ordering on the categories. Instead of representing a geological model by  $\mathbf{m} : R^3 \rightarrow \mathbb{N}$  we introduce an encoded vector function

$$\mathbf{m}^{(oh)} : R^3 \rightarrow [0, 1]^{\mathbb{N}}, \quad (6)$$

such that each integer value of  $\mathbf{m}$  is mapped to a new vector. The new function,  $\mathbf{m}^{(oh)}$ , represents the likelihood of a point  $\mathbf{x}$  in our model to belong to a particular class that ranges from 1 to  $\mathbb{N}$ . The vector function  $\mathbf{m}_i^{(oh)}(\mathbf{x})$  is sometimes referred to as the one-hot encoding of the model  $\mathbf{m}$ .

We further normalize these embedding vectors to have an unweighted mean of zero and unit length such that

$$\mathbf{m}_i^{(e)} = \frac{\mathbf{m}_i^{(oh)} - \left(\frac{1}{N}, \dots, \frac{1}{N}\right)}{\|\mathbf{m}_i^{(oh)} - \left(\frac{1}{N}, \dots, \frac{1}{N}\right)\|}. \quad (7)$$

Because we no longer require each embedding vector to remain on the probability simplex, the flow field is free to traverse an unconstrained continuous space. It is then the task of the model to learn the probability distribution  $\pi_{\mathbf{m}^{(e)}}$  in the embedded space, from which we can decode back to the original categorical space of  $\mathbf{m}$ . To decode a voxel  $x^{(e)}$  back to a discrete category, we select the embedding vector  $\mathbf{m}_i^{(e)}$  with the largest cosine similarity:

$$i = \arg \max_i \langle x^{(e)}, \mathbf{m}_i^{(e)} \rangle. \quad (8)$$

**Flow Matching** Flow matching is a powerful technique that can be used to connect any two probability spaces. We define the distributions,  $\mathbf{m}_t^{(e)}$  by

$$\mathbf{m}_t^{(e)}(\mathbf{x}) = t\mathbf{m}^{(e)}(\mathbf{x}) + (1-t)\mathbf{z}, \quad (9)$$

where  $\mathbf{z} \sim N(0, \mathbf{I})$ . Flow matching learns the velocity field  $\mathbf{v} = d/dt \left( \mathbf{m}_t^{(e)}(\mathbf{x}) \right) = \mathbf{m}^{(e)}(\mathbf{x}) - \mathbf{z}$  characterized by the unique minimizer of the quadratic objective

$$\min_{\xi} \frac{1}{2} \mathbb{E}_{t, \mathbf{z}} \left\| \mathbf{v}(\mathbf{m}_t^{(e)}, t; \xi) - \mathbf{m}^{(e)}(\mathbf{x}) + \mathbf{z} \right\|^2. \quad (10)$$

Here  $\mathbf{v}(\mathbf{m}_t^{(e)}, t; \xi)$  is a neural network model that takes  $\mathbf{m}_t^{(e)}$  and  $t$  as inputs and parameterized by  $\xi$ . The parameters  $\xi$  are adjusted to solve the optimization problem, and this is done through stochastic gradient descent.

While in standard training of generative models, the data set is finite and static, our data set is practically infinite and dynamic. This stems from the ability to generate models "on the fly" as the system is being generated, allowing for a diverse set of models to train the system.

## Applications

A trained model  $\mathbf{v}(\mathbf{m}_t, t; \xi)$  indirectly learns the distribution  $\pi_{\mathbf{m}}$ , allowing us to draw or infer new geological models that are similar to the training set. Generating arbitrary samples from  $\pi_{\mathbf{m}}$  is an example of unconditional generation where the flow process is not guided or conditioned by any constraints. To draw a new sample, we integrate the learned ODE using a numerical solver such as Runge-Kutta or adaptive Heun's method,

$$\frac{d\mathbf{m}}{dt} = \mathbf{v}(\mathbf{m}_t, t; \xi) \quad \mathbf{m}(0) = \mathbf{m}_0 \sim N(0, \mathbf{I}) \quad t \in [0, 1]. \quad (11)$$

While the unconditional generation of models is helpful in many applications where models are needed for the simulation of other data (see, e.g.,<sup>30</sup>), a more important application is the integration of measured data. Consider some noisy data of the form

$$\mathbf{d} = \mathbf{A}\mathbf{m} + \boldsymbol{\epsilon}, \quad (12)$$

where  $\mathbf{A}$  is the so called forward mapping and  $\boldsymbol{\epsilon} \sim N(0, \sigma^2 \mathbf{I})$  is the noise.

There are a number of ways to integrate the measured data into the ODE system, Note that equation equation 12 is an algebraic constraint that is added to the ordinary differential equation. This changes the ODE into a Differential Algebraic Equation (DAE)<sup>31</sup>. The incorporation of such constraints in the context of deep learning was recently discussed in<sup>32</sup>. A straightforward approach is adding a term to the ODE that "attracts" the solution of the ODE toward the data, obtaining the system

$$\frac{d\mathbf{m}}{dt} = \mathbf{v}(\mathbf{m}_t, t; \boldsymbol{\xi}) - \mu \mathbf{A}^\top (\mathbf{A}\mathbf{m} - \mathbf{d}) \quad \mathbf{m}(0) = \mathbf{m}_0 \sim N(0, \mathbf{I}) \quad t \in [0, 1]. \quad (13)$$

The parameter  $\mu$  balances between data fit and fit to the prior model and is tuned typically by cross-validation. For a general application of conditional data to the generation process, we add an additional embedding of conditional data  $\mathbf{d}$  to the machine learning model and a modification to the loss function using a method adapted from recent work by Ahamed and Haber<sup>33</sup>. Ultimately, the goal is to learn to sample from the distribution  $\pi_{\mathbf{m}}(\mathbf{m}|\mathbf{d})$  to produce many different candidate geological models for a set of field data.

## Results

### Unconditional Generation of Earth Models

In our first set of experiments, we show that a flow matching model trained with suitable synthetic data in a continuously embedded space can generate realistic Earth models. Unconditional generation is carried out using the learned velocity flow field and a numerical ODE solver<sup>34</sup>. After integration, the resulting sample is decoded into the categorical space. Figure 3 highlights three example models produced with this approach.

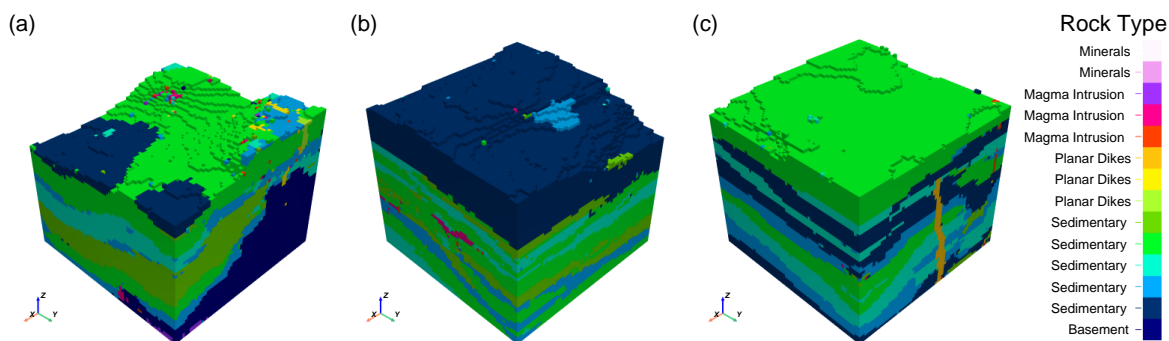


**Figure 3. Three examples of unconditional Earth models.** Panels (a–c)  $64 \times 64 \times 64$  resolution generative samples using flow matching. Each model represents a  $3.84 \text{ km} \times 3.84 \text{ km} \times 3.84 \text{ km}$  volume of the Earth’s crust.

These models are diverse and include different topography, layer thickness, layer geometry, as well as dykes and intrusions. Such samples can support data generation<sup>30</sup> for various applications as discussed in<sup>35,36</sup> as well as for training other machine learning tasks such as geological segmentation and mapping<sup>37</sup>, or classification<sup>38</sup>.

### Conditional Generation of Earth Models

In our next experiment, we demonstrate how conditional generation can be used for a common but important task: geological interpolation of lithology from borehole data. The procedure entails constructing 3D subsurface models from sparse, irregularly sampled borehole data. This task bridges observed lithological measurements (e.g., sand, clay, shale) with geostatistical or simulation-based techniques to predict the unobserved subsurface composition. Such a problem is commonly solved to create initial models for reservoir characterization, groundwater flow analysis, or contaminant transport studies.

The standard technique for solving this problem is kriging<sup>39</sup> and, more recently, interval kriging<sup>40</sup>, which estimates lithological probabilities between boreholes by accounting for vertical and horizontal variability in rock types. However, kriging can struggle when the data size is small (few boreholes) and has the tendency to smooth interfaces when applied to categorical data. We demonstrate an alternative reconstruction method using a conditional flow matching model to interpolate between sparse boreholes. Because the technique is inherently generative, we can produce many different models that are consistent with the observed data and also with the underlying probability density function of the model.

To guide this example, we extract the observable surface data and sparse boreholes from a Geomodel that was never seen during training and use the original model as a ground truth benchmark. Shown in Figure 4 are the original mode, the surface data, and 25 boreholes for the experiments that follow.

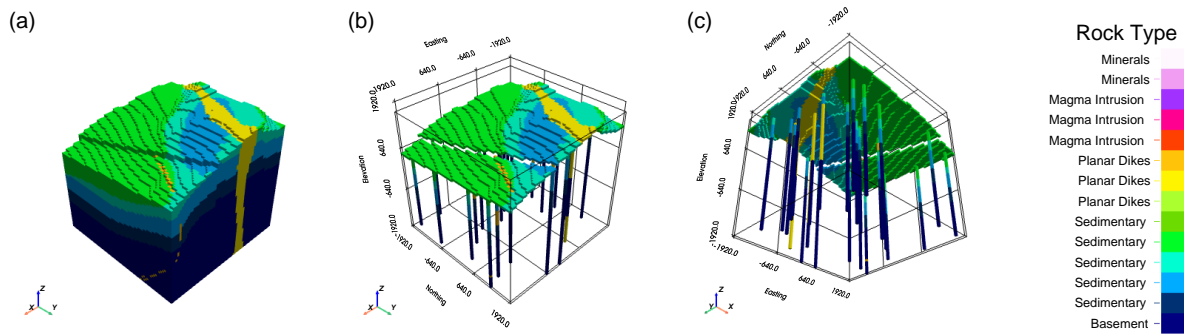


**Figure 4.** (a) A 3D Geomodel unseen during training is used to produce sparse conditional data for reconstruction in (b) and (c) consisting of 25 randomly placed vertical boreholes one single  $(60 \times 60 \times 60)\text{m}^3$  voxel in diameter.

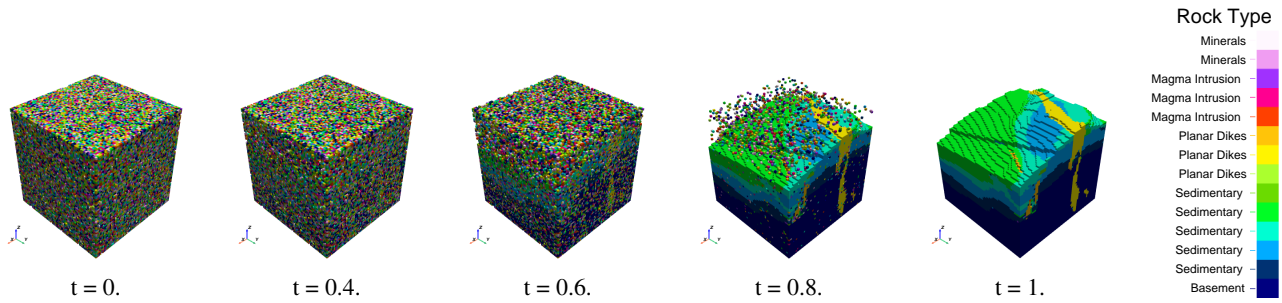


**Figure 5.** A sequential visualization of the model shows the generative process that maps from Gaussian noise to plausible geology conditioned on sparse data. Decoded models in the discrete categorical space from intermediary distributions between  $t = 0$  to  $t = 1$  show snapshots from a continuous flow bridging between a Gaussian distribution and  $\pi_{\mathbf{m}}(\mathbf{m}|\mathbf{d})$ .

The surface data and boreholes are used to guide the flow process using a set of different starting seeds consisting of Gaussian noise drawn from a normal distribution, shown in Figure 5.

Each instance of Gaussian noise maps to a different reconstruction conditioned on the sparse data, offering complete reconstructions of hypothetical yet probable geology, a technique referred to as inpainting. Three such volumetric realizations are shown in Figure 6. While the models are identical at the ground surface where conditional information was fully specified, they diverge in areas that were not covered by the conditional data, for example, the extent and shape of the two planar dike features.

### Conditional Feature Estimation and Reconstruction

Individual features of a reconstructed model, such as dike formations, can be analyzed in greater detail using an ensemble of samples from the conditional distribution  $\pi_{\mathbf{m}}(\mathbf{m})$ . The planar dikes in the original model, the sparse dike data, and several reconstructions of their form are shown in Figure 7. The realizations show a high degree of variability due to the very limited conditional data.

A large ensemble of samples can be used as a probability estimate for the likelihood of any individual voxel being part of the larger dike structure. A pattern emerges when plotting the extent of the planar dike based on the contour shape of probabilistic confidence intervals. Shown in Figure 8, a lower confidence interval corresponds to a larger and more aggressive extrapolation range from the existing boreholes. The smaller dike shown in the model has insufficient conditional data to produce an accurate reconstruction, a problem exacerbated by the true extent of the dike being largely obscured by sediment.

### Discussion

Our results demonstrate the feasibility and potential of using generative artificial intelligence (AI) models, particularly flow matching techniques, to construct realistic and geologically plausible three-dimensional structural models. The work presented here integrates two key components. First, we construct a process for creating a large, synthetic, and geologically consistent dataset that seeks to embed the rich and complex knowledge of structural geology into a mathematical framework suitable for training machine learning models. Second, we train a generative AI model that implicitly learns both unconditional and conditional probability distributions of geological structures. By doing so, it efficiently captures essential characteristics of the

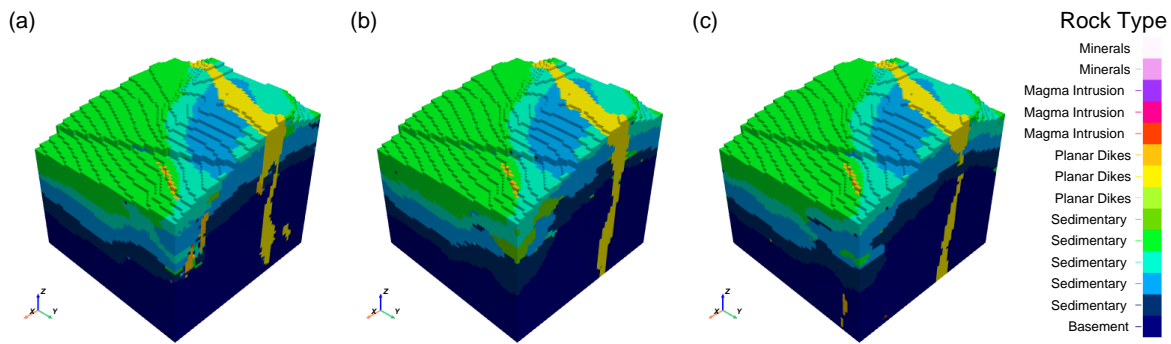


**Figure 6.** Three geological models from  $\pi_{\mathbf{m}}(\mathbf{m}|\mathbf{d})$  via numerical integration conditioned on available lithological data. The models offer a complete 3D ( $64 \times 64 \times 64$ ) resolution reconstruction, with the exterior surface of the models shown here for comparison.

Earth's crust and provides a highly complex prior to tackle the challenges common in geoscience applications, including data sparsity, uncertainty quantification, and the integration of diverse data modalities.

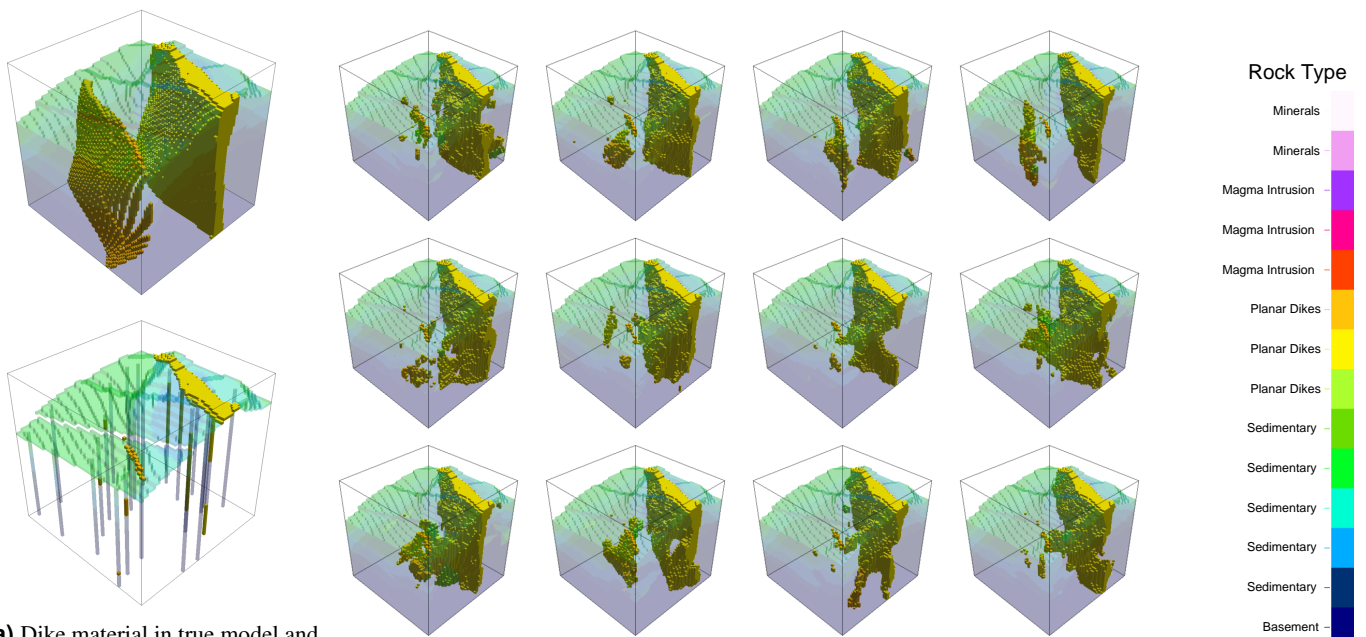
**Advancements in Generative Modeling for Structural Geology.** Generative AI for structural geology offers a significant advantage over traditional deterministic approaches through their capacity to define multiple plausible geological realizations, which is particularly valuable for the ill-posedness of geological reconstruction from often sparse and incomplete data. The use of synthetic data to train a generative model is an opportunity to specify prior knowledge that is vastly more complex than what would be permitted through classical techniques such as regularization. The unconditional models generated have a high degree of geological diversity, capturing variations in topography, layer geometry, and structural features such as dykes and intrusions. This type of synthetic modeling has numerous applications, including data augmentation for training machine learning models, benchmarking geophysical inversion algorithms, and enhancing geostatistical modeling techniques. Our results further reinforce previous studies that highlight the importance of generative approaches in geosciences<sup>30,35,36,41</sup>.

**Conditional Modeling, Reconstruction, and Uncertainty Quantification.** The ability to generate samples conditioned on sparse borehole data presents a major breakthrough for geological interpolation tasks. The technique can succeed where tools such as kriging often struggle, for example, when borehole data is limited or categorical. The generative model approach produces an ensemble of realizations that not only fit the observed data but also adhere to a probability distribution of plausible geology encoded into the synthetic training set. The generated models are not only consistent with the conditional data but also diverse, assisting tasks such as risk assessment and decision-making in resource exploration, subsurface engineering, and geological hazard analysis. By providing a suite of possible geological scenarios, our approach allows decision-makers to incorporate uncertainty into their models rather than relying on a single deterministic solution.

**Implications and Future Directions.** The ability to generate diverse, geologically plausible models has far-reaching implications for a variety of geoscientific applications. One promising direction is the integration of our generative framework with geophysical inversion workflows, where subsurface properties inferred from geophysical data can be used to further constrain model realizations. Additionally, combining our approach with Bayesian inference techniques could enable probabilistic geological modeling, providing a more rigorous quantification of uncertainty.

**Conclusions.** The incorporation of generative AI into structural geology represents a paradigm shift, enabling more flexible, data-driven, and probabilistic interpretations of the Earth's subsurface. As these methods continue to evolve, they have the potential to transform geological modeling, supporting improved resource exploration through, e.g., providing novel types of regularization for geophysical inverse problems, as well as geohazard assessment and geotechnical decision-making.

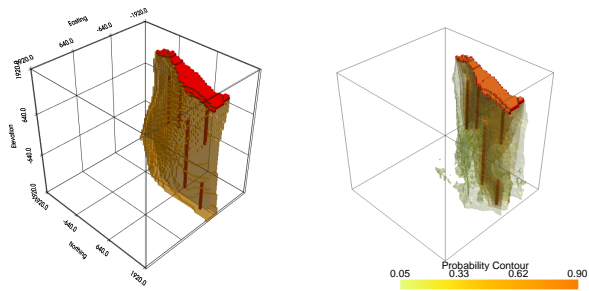
Finally, while this study represents a significant step toward automation in structural geology, human expertise remains invaluable. Rather than replacing traditional geological interpretation, our approach should be viewed as a powerful tool that enhances geologists' ability to explore multiple hypotheses, validate models, and make informed decisions in the face of uncertainty.



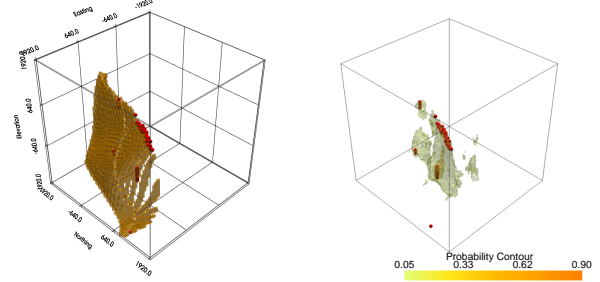
**(a)** Dike material in true model and conditional data.

**(b)** 12 different dike realizations conditioned on surface and borehole data.

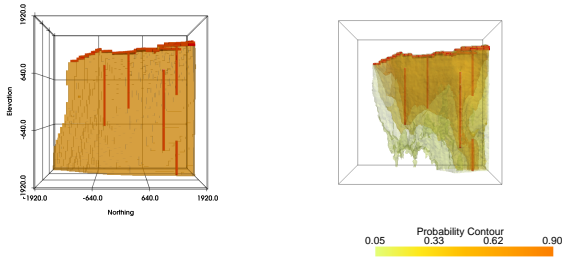
**Figure 7. Comparison of conditioned dike realizations.** In (a), the true shape of two geological dikes is shown, along with the sparse data sampled from surface and borehole data. (b) Many conditional realizations of the subsurface dike distribution are estimated by sampling from the generative model with the conditional data.



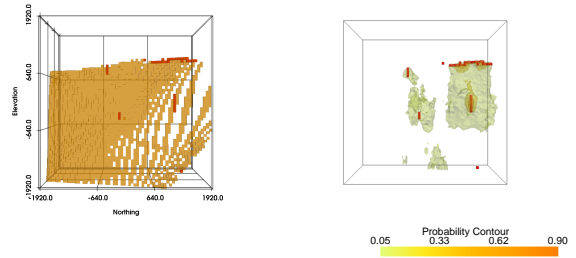
(a) Dike 1 probability map, isometric.



(b) Dike 2 probability map, isometric.



(c) Dike 1 probability map, front view.



(d) Dike 2 probability map, front view.

**Figure 8. Comparison of conditional dike realizations.** Two dike reconstructions from sparse data at different probability confidence intervals. In each subfigure, on the left is the true dike, which is shown in gold, with sparse field data shown in red. On the right is a probability estimate using an ensemble of 100 conditional reconstructions from the generative flow model. Four different probability thresholds are shown: 5%, 33%, 62%, and 90%.

## References

1. Fossen, H. *Structural geology* (Cambridge University Press, 2016).
2. Park, R. *Foundation of structural geology* (Routledge, 2013).
3. McClay, K. R. *The mapping of geological structures* (John Wiley & Sons, 2013).
4. Wellmann, F. & Caumon, G. Chapter One - 3-D Structural geological models: Concepts, methods, and uncertainties. In Schmelzbach, C. (ed.) *Advances in Geophysics*, vol. 59, 1–121, DOI: [10.1016/bs.agph.2018.09.001](https://doi.org/10.1016/bs.agph.2018.09.001) (Elsevier, 2018).
5. Karpatne, A., Ebert-Uphoff, I., Ravela, S., Babaie, H. A. & Kumar, V. Machine Learning for the Geosciences: Challenges and Opportunities. *IEEE Transactions on Knowl. Data Eng.* **31**, 1544–1554, DOI: [10.1109/TKDE.2018.2861006](https://doi.org/10.1109/TKDE.2018.2861006) (2019).
6. Wellmann, J. F., Horowitz, F. G., Schill, E. & Regenauer-Lieb, K. Towards incorporating uncertainty of structural data in 3d geological inversion. *Tectonophysics* **490**, 141–151 (2010).
7. Calcagno, P., Chilès, J.-P., Courrioux, G. & Guillen, A. Geological modelling from field data and geological knowledge: Part i. modelling method coupling 3d potential-field interpolation and geological rules. *Phys. Earth Planet. Interiors* **171**, 147–157 (2008).
8. Wellmann, F. & Caumon, G. 3-d structural geological models: Concepts, methods, and uncertainties. In *Advances in Geophysics*, vol. 59, 1–121 (Elsevier, 2018).
9. Houlding, S. *3D geoscience modeling: Computer techniques for geological characterization* (Springer Science & Business Media, 2012).
10. Albergo, M. S., Boffi, N. M. & Vanden-Eijnden, E. Stochastic Interpolants: A Unifying Framework for Flows and Diffusions (2023). [2303.08797](https://arxiv.org/abs/2303.08797).
11. Lipman, Y., Chen, R. T., Ben-Hamu, H., Nickel, M. & Le, M. Flow matching for generative modeling. In *ICLR 2023* (2023). ArXiv preprint [arXiv:2210.02747](https://arxiv.org/abs/2210.02747).
12. Yang, L. *et al.* Diffusion models: A comprehensive survey of methods and applications. *ACM Comput. Surv.* (2022).
13. Deng, J. *et al.* ImageNet: A Large-Scale Hierarchical Image Database. In *CVPR09* (2009).
14. Hadid, A., Chakraborty, T. & Busby, D. When Geoscience Meets Generative AI and Large Language Models: Foundations, Trends, and Future Challenges (2024). [2402.03349](https://arxiv.org/abs/2402.03349).
15. GM, H., Gourisaria, M. K., Pandey, M. & Rautaray, S. S. A comprehensive survey and analysis of generative models in machine learning. *Comput. Sci. Rev.* **38**, 100285, DOI: <https://doi.org/10.1016/j.cosrev.2020.100285> (2020).
16. Ruthotto, L. & Haber, E. An introduction to deep generative modeling. *GAMM-Mitteilungen* **44**, e202100008, DOI: [10.1002/gamm.202100008](https://doi.org/10.1002/gamm.202100008) (2021).
17. Lienen, M., Lüdke, D., Hansen-Palmus, J. & Günemann, S. From zero to turbulence: Generative modeling for 3d flow simulation. *arXiv preprint arXiv:2306.01776* (2023).
18. Li, S. *et al.* Globaltomo: A global dataset for physics-ML seismic wavefield modeling and FWI. *arXiv preprint arXiv:2406.18202* (2024).
19. Goshisht, M. K. Machine learning and deep learning in synthetic biology: Key architectures, applications, and challenges. *ACS omega* **9**, 9921–9945 (2024).
20. Jones, N. The AI revolution is running out of data. what can researchers do? *Nature* **636**, 290–292, DOI: [10.1038/d41586-024-03990-2](https://doi.org/10.1038/d41586-024-03990-2) (2024).
21. de la Varga, M., Schaaf, A. & Wellmann, F. Gempy 1.0: open-source stochastic geological modeling and inversion. *Geosci. Model. Dev.* **12**, 1–32, DOI: [10.5194/gmd-12-1-2019](https://doi.org/10.5194/gmd-12-1-2019) (2019).
22. Jessell, M. W. Noddy – an interactive map creation package. Unpublished MSc Thesis (1981).
23. Jessell, M. *et al.* Into the Noddyverse: a massive data store of 3D geological models for machine learning and inversion applications. *Earth Syst. Sci. Data* **14**, 381–392, DOI: [10.5194/essd-14-381-2022](https://doi.org/10.5194/essd-14-381-2022) (2022).
24. Grose, L., Ailleres, L., Laurent, G. & Jessell, M. LoopStructural 1.0: time-aware geological modelling. *Geosci. Model. Dev.* **14**, 3915–3937, DOI: [10.5194/gmd-14-3915-2021](https://doi.org/10.5194/gmd-14-3915-2021) (2021). Publisher: Copernicus GmbH.
25. Cockett, R., Moran, T. & Pidlisecky, A. Visible geology: Creative online tools for teaching, learning, and communicating geologic concepts (2016).
26. Modersitzki, J. *Numerical Methods for Image Registration* (Oxford, 2004).

27. Chung, H., Sim, B. & Ye, J. C. Come-closer-diffuse-faster: Accelerating conditional diffusion models for inverse problems through stochastic contraction. In *Proceedings of the IEEE/CVF Conference on Computer Vision and Pattern Recognition*, 12413–12422 (2022).
28. Meng, C., Choi, K., Song, J. & Ermon, S. Concrete score matching: Generalized score matching for discrete data. *Adv. Neural Inf. Process. Syst.* **35**, 34532–34545 (2022).
29. Hyvärinen, A. Some extensions of score matching. *Comput. statistics & data analysis* **51**, 2499–2512 (2007).
30. Wellmann, F., Thiele, S., Lindsay, M. & Jessell, M. Pynoddy 1.0: An experimental platform for automated 3-D kinematic and potential field modelling. *Geosci. Model. Dev. Discuss.* **8**, 10011–10051, DOI: [10.5194/gmdd-8-10011-2015](https://doi.org/10.5194/gmdd-8-10011-2015) (2015).
31. Ascher, U. M. & Petzold, L. R. *Computer methods for ordinary differential equations and differential-algebraic equations*, vol. 61 (Siam, 1998).
32. Boesen, T., Haber, E. & Ascher, U. M. Neural daes: Constrained neural networks. *SIAM J. on Sci. Comput.* **47**, C291–C312 (2025).
33. Ahamed, S. & Haber, E. DAWN-FM: Data-Aware and Noise-Informed Flow Matching for Solving Inverse Problems, DOI: [10.48550/ARXIV.2412.04766](https://doi.org/10.48550/ARXIV.2412.04766) (2024).
34. Chen, R. T. Q. torchdiffeq (2018). <https://github.com/rtqichen/torchdiffeq>.
35. Woollam, J. *et al.* Seisbench – a toolbox for machine learning in seismology (2021). [2111.00786](https://doi.org/10.2111/00786).
36. Bednar, J. B., Abriél, W. L., Biondi, B. L., Levin, S. A. & Cheng, A. C. H. SEG Advanced Modeling (SEAM) today and tomorrow. *Seg Tech. Program Expand. Abstr.* (2006).
37. Julka, S. & Granitzer, M. Knowledge distillation with segment anything (sam) model for planetary geological mapping (2023). [2305.07586](https://doi.org/10.2305.07586).
38. Zhang, Y., Wang, G., Li, M. & Han, S. Automated classification analysis of geological structures based on images data and deep learning model. *Appl. Sci.* **8** (2018).
39. Stein, M. L. *Interpolation of spatial data*. Springer Series in Statistics (Springer-Verlag, New York, 1999).
40. Song, Y. & Tsai, F. T.-C. Borehole-based interval kriging for 3d lithofacies modeling. *Water Resour. Res.* **60**, e2023WR035020 (2024).
41. Bergen, K. J., Johnson, P. A., De Hoop, M. V. & Beroza, G. C. Machine learning for data-driven discovery in solid Earth geoscience. *Science* **363**, eaau0323, DOI: [10.1126/science.aau0323](https://doi.org/10.1126/science.aau0323) (2019).

## Author contributions statement

S.G. developed the synthetic data set generator and was involved in the generative AI model development. V.O. and S.Z. trained the foundation model. G.T. led the training and together with D.K. organized the KAUST-based effort. E.H. conceived of and led the overall project. All authors participated in preparing and reviewing the manuscript.

## Additional information

**Accession codes:** The custom streaming synthetic data generator *StructuralGeo* used in this study is available at: <https://github.com/eldadHaber/StructuralGeo/releases/tag/v1.0>, with an archived version deposited at Zenodo: <https://doi.org/10.5281/zenodo.15244035>. The generative AI model code used in selected experiments is available at: [https://github.com/chipnbits/flowtrain\\_stochastic\\_interpolation/releases/tag/v1.0.0](https://github.com/chipnbits/flowtrain_stochastic_interpolation/releases/tag/v1.0.0).

**Competing Interests Statement:** The authors declare no competing interests.